

# Infrared and EPR Spectroscopic Studies of 2-C<sub>2</sub>H<sub>2</sub>F and 1-C<sub>2</sub>H<sub>2</sub>F Radicals Isolated in Solid Argon

I. U. Goldschleger,\* A. V. Akimov,\* E. Ya. Misochnko,\* and C. A. Wight†

\*Institute of Problems of Chemical Physics of the Russian Academy of Sciences, 142432, Chernogolovka, Moscow region, Russian Federation; and

†Department of Chemistry, University of Utah, Salt Lake City, Utah 84112

E-mail: [ilya@icp.ac.ru](mailto:ilya@icp.ac.ru), [wight@chem.utah.edu](mailto:wight@chem.utah.edu)

Received August 17, 2000; in revised form October 12, 2000

2-fluorovinyl radicals were generated in solid argon by solid-state chemical reactions of mobile F atoms with acetylene and its deuterated analogues. Highly resolved EPR spectra of the stabilized radicals CHF=·CH, CDF=·CD, CHF=·CD, and CDF=·CH were obtained for the first time. The observed spectra were assigned to *cis*-2-fluorovinyl radical based on excellent agreement between the measured ( $a_F = 6.50$ ,  $a_{\text{BH}} = 3.86$ ,  $a_{\text{aH}} = 0.25$  mT) hyperfine constants and those calculated using density functional (B3LYP) theory. Analogous experiments carried out using infrared spectroscopy yielded a complete assignment of the vibrational frequencies. An unusual reversible photochemical conversion is observed in which *cis*-2-fluorovinyl radicals can be partially converted to 1-fluorovinyl radicals by pulsed laser photolysis at 532 nm. Photolysis at 355 nm converts 1-fluorovinyl back to *cis*-2-fluorovinyl. High-resolution EPR and infrared spectra of 1-fluorovinyl were obtained for the first time. The measured hyperfine constants ( $a_F = 13.71$ ,  $a_{\text{H1}} = 4.21$ ,  $a_{\text{H2}} = 1.16$  mT) are in good agreement with calculated values. © 2001 Academic Press

**Key Words:** cryochemistry; EPR; infrared spectroscopy; fluorine; acetylene; 2-fluorovinyl radical; 1-fluorovinyl radical.

## INTRODUCTION

Free radicals play an important role in many chemical and biological processes. Therefore considerable attention has been given to study of their properties (1). The matrix isolation technique has been a highly successful method for spectroscopic investigations of radical products of chemical reactions. A common variant of this method is to trap gas-phase reaction products and freeze them in a matrix consisting of a large excess of argon or neon. The relatively weak guest–host interactions allow spectroscopic characterization of the matrix-isolated species under conditions that are similar to the gas phase but at much higher density than can ordinarily be achieved in the gas phase.

Infrared absorption and EPR spectra of many radicals were obtained using this technique and received general acceptance (2). However, in some cases, radicals were misidentified or poorly characterized. In particular, difficulties in their identification by IR spectroscopy included (a) the presence of secondary gas-phase reaction products; (b) stabilization of products in different structural traps of the solid matrix results in multiple infrared bands, or “site splittings”; (c) registration of low-frequency IR bands  $\nu \leq 300 \text{ cm}^{-1}$ , which are required for reliable identification of radical-molecular complexes, structural isomers, or conformational isomers, is experimentally challenging under ordinary conditions.

Most of these difficulties can be overcome if the radicals are generated by atom–molecular reactions that take place directly

in the matrix. The most challenging aspect of this method is that reactants are normally closed-shell species; therefore, most of the likely reaction products will also be closed-shell. However, we have recently explored a modification of the method that is based on the high mobility of fluorine atoms in rare gas matrices and on the combination of two complementary spectroscopic techniques, IR and EPR (3, 4). The ability of fluorine atoms (e.g., generated by photolysis of F<sub>2</sub>) to migrate in solid argon over long distances (5, 6) allows them to react with closed-shell species to form free radicals at sufficiently high concentrations for spectroscopic study. The advantages of using of two complementary spectroscopic techniques (EPR for sensitive detection of radicals and IR for characterization of closed-shell products) were demonstrated earlier for reactions of fluorine atoms with methane (3), ethylene (7), nitrogen oxide (8), and ammonia (4).

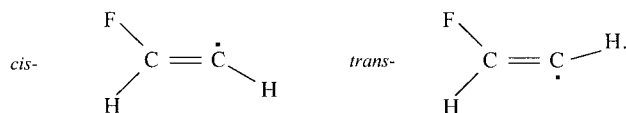
Using this approach, we have shown that complete sets of isotropic hyperfine constants (hf) can be determined from high-resolution EPR spectra of radicals in solid argon. Theoretically calculated isotropic hf constants of radicals and radical-molecular complexes are generally in good agreement with those measured. The isotropic hf constants change drastically upon even minor distortion from the equilibrium geometry, whereas vibrational frequencies generally do not (3). Therefore EPR technique is a more reliable method for identification and clarification of the structure and geometry of stabilized radicals than the infrared technique. The main advantage of using IR is that most of the

molecules can be detected, providing a more comprehensive probe of reactants and products.

This paper is devoted to the study of fluorovinyl radicals formed in the reactions of mobile F atoms with  $C_2H_2$  molecules. In the gas phase, this reaction leads to the formation of two types of products:



It was determined that the dominant channel is the formation of  $2-C_2H_2F$  radical (9, 10). There are two isomers of this radical, which differ in the location of the F atom with respect to the orbital of unpaired electron:



The first attempt to obtain the EPR spectrum of  $\beta-C_2D_2F$  radical by  $F_2$  photolysis of solid ternary mixtures  $Ar/F_2/C_2D_2$  at 4.2 K was made in 1970 by Cochran *et al.* (11). They observed a poorly resolved anisotropic spectrum, but they were able to determine isotropic hf constants for the F atom ( $a_F = 6.9$  mT) and deuterium ( $a_D = 0.6$  mT). Based on the known isotropic hf constants of both isomers of  $C_2H_3$  radical (12), they ascribed the detected EPR spectrum to *trans*- $\beta-C_2D_2F$  radical. Better-resolved spectra of 2-fluorovinyl radical in an  $SF_6$  matrix were obtained by Shiotani *et al.* (13). These authors also assigned the observed spectra to *trans*- $2-C_2H_2F$  radical. Such assignment was based on the results of semiempirical INDO MO calculations, which predicted that *trans* isomer is more stable than the *cis* isomer. The infrared absorption spectrum of matrix-isolated fluorovinyl radical was reported by Jacox (14) by trapping the gas-phase products of the  $F + C_2H_2$  reaction. Many different species were generated in this experiment, and it required exceptional skill and scrupulousness to separate the infrared bands of  $2-C_2H_2F$  radical from the variety of other bands. Jacox obtained a reasonable fit of the isotopic data to a diagonal valence force field potential using the assumed structure of *trans*- $2-C_2H_2F$  radical, and with the support of the previous EPR study (11), she assigned the observed spectrum to *trans*- $2-C_2H_2F$ .

The first reliable calculations of spectroscopic characteristics of fluorovinyl radicals performed with post-Hartree-Fock methods and density functional methods appeared in 1993 (15). These calculations showed that the energy of the *cis* isomer is lower than the *trans* isomer when the basis set is enlarged and differences in zero-point vibrational energy are taken into account. The spin density in the  $2-C_2H_2F$  radical is qualitatively different from that of  $C_2H_3$ , thereby casting some doubt on Cochran's original assignment. The isotropic hf constants of *cis* and *trans* isomers of  $2-C_2H_2F$  strongly differ from

each other, and the measured hf constants (11, 13) are actually close to those calculated for *cis*- $2-C_2H_2F$ . The calculated harmonic vibrational frequencies of both isomers are nearly the same (i.e., the differences in the frequencies are comparable with the accuracy of calculations).

In this paper, we show how it is possible to form relatively high concentrations of isolated fluorovinyl radicals at 24 K by reaction of thermally diffusing F atoms with matrix-isolated acetylene molecules. We make a definitive assignment of the spectroscopic properties of *cis*- $2-C_2H_2F$  based on an experimental approach (4, 8) that combines measurements made using infrared and EPR spectroscopies. The correlation of the results is made possible by the discovery of a reversible photoconversion between *cis*- $2-C_2H_2F$  and  $1-C_2H_2F$  that is observed in both types of experiments.

## EXPERIMENTAL

The experimental techniques are similar to those used in our previous studies (3). Samples were prepared by vacuum co-deposition of gaseous mixtures  $Ar/C_2H_2$  and  $Ar/F_2$  onto a substrate (CsI salt window in IR experiments, or a sapphire rod in the EPR experiments) maintained at 15 K. The composition of typical samples was  $Ar:F_2:C_2H_2 = 3000:1:1$ , though the relative concentration of reactants were varied from  $3 \times 10^{-3}$  to  $2.5 \times 10^{-4}$ . The thickness of the samples was approximately 100  $\mu m$ .

The EPR experiments were carried out with a homemade helium flow cryostat with a movable helium shaft (3). The temperature stability was  $\sim 0.1$  K over the range 15–40 K. EPR spectra were recorded using standard 9 GHz spectrometer. Infrared spectra were recorded with a Mattson Model RS/10000 FTIR spectrometer (spectral region from 500 to 4000  $cm^{-1}$  and spectral resolution 0.5  $cm^{-1}$ ). The closed-cycle helium refrigerator (APD Cryogenics Model DE-202) was used to maintain the sample temperature in these experiments. In a separate experiment we verified that the light from the ceramic global source did not induce any chemical reactions.

Fluorine atoms were generated by  $F_2$  photolysis at  $\lambda = 355$  nm (third harmonic of Nd:YAG laser in IR experiments) and  $\lambda = 337$  nm ( $N_2$  laser in EPR experiments). The average power did not exceed 10  $mW/cm^2$  in either type of experiment. To distinguish the chemical reactions involving photogenerated F atoms from those of diffusing thermal atoms, photolysis of  $F_2$  molecules was performed at 15 K. Fluorine atoms are able to diffuse in solid argon at temperatures above 20 K. To initiate reactions of thermal F atoms, we performed annealing of photolyzed samples at 24 K. Annealing was carried out by step-by-step procedure. After completion of photolysis at 15 K, the sample was annealed 3–5 min at 24 K. Then the temperature was lowered back to 15 K and the spectrum was recorded. This cycle were repeated 10–12 times until reactions were complete.

UV photolysis at 15 K and subsequent annealing of an  $Ar/F_2$

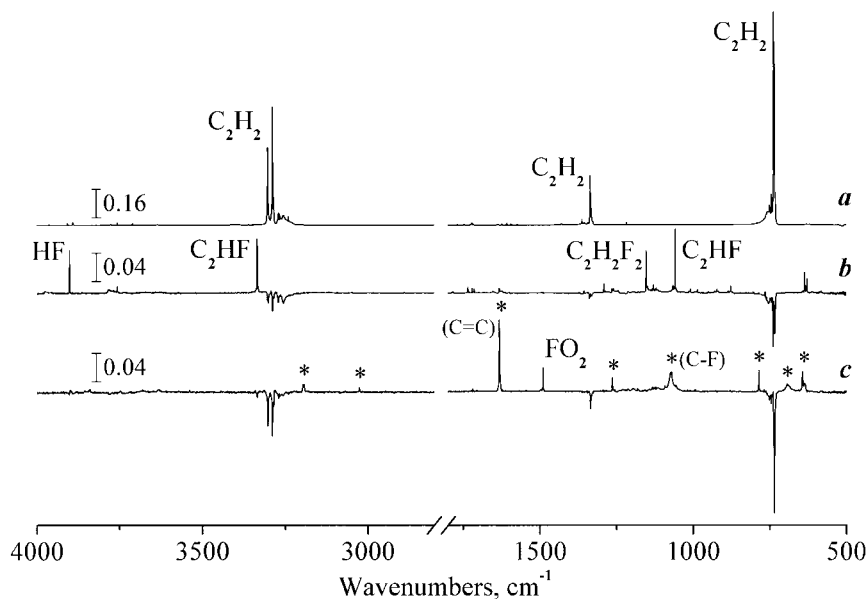


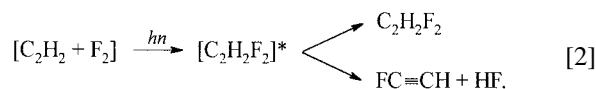
**FIG. 1.** Infrared spectra of a sample Ar:F<sub>2</sub>:C<sub>2</sub>H<sub>2</sub> = 3000:1:1 after deposition (trace a). Difference spectrum after exhaustive UV photolysis at 15 K (trace b). Trace c shows difference spectrum of photolyzed sample before and after annealing at 24 K. IR bands of 2-C<sub>2</sub>H<sub>2</sub>F are marked with asterisks. All spectra were recorded at 15 K.

sample at 24 K lead to the appearance of a sharp absorption at 1490 cm<sup>-1</sup> in the infrared spectrum corresponding to FO<sub>2</sub> radicals. In the similar EPR studies the spectrum of this radical is also observed. Molecular oxygen is a common impurity in fluorine gas and is difficult to remove by fractional distillation. Therefore oxygen is always present in the samples in small concentration ~10<sup>-4</sup>–10<sup>-5</sup>. Since diffusing fluorine atoms react with O<sub>2</sub> molecules to form FO<sub>2</sub> radicals (16), we have used this reaction as an internal standard for characterizing the reaction rate of diffusing F atoms during the annealing cycles. EPR spectra of freshly prepared Ar:C<sub>2</sub>H<sub>2</sub>:F<sub>2</sub> samples exhibit no lines due to paramagnetic species. Very weak infrared bands of CO<sub>2</sub> (661.9, 2340.5 cm<sup>-1</sup>) are observed in the IR spectra of deposited samples.

## RESULTS AND DISCUSSION

### A. Infrared Absorption Spectra of 2-C<sub>2</sub>H<sub>2</sub>F Radicals

The IR spectrum of Ar:F<sub>2</sub>:C<sub>2</sub>H<sub>2</sub> = 3000:1:1 after deposition is shown in Fig. 1a. It contains broad bands of acetylene with maxima at 736.5, 1334.5, and 3288.5 (3302.0) cm<sup>-1</sup>. Brief UV photolysis (~5 min) at 15 K leads to rapid growth of intense bands in the regions of C—F stretching vibration (1058, 1129, and 1153 cm<sup>-1</sup>) and HF molecular vibration (3756 and 3900 cm<sup>-1</sup>) (see Fig. 1b). These bands are attributed to C<sub>2</sub>H<sub>2</sub>F<sub>2</sub> and a molecular complex of C<sub>2</sub>H<sub>2</sub>F bound to HF (17, 18). Such molecular products could be generated in the cage reaction by photolysis of the complex of reactants [C<sub>2</sub>H<sub>2</sub> + F<sub>2</sub>]:



After prolonged photolysis, the C<sub>2</sub>H<sub>2</sub> bands are reduced by ~2%; this corresponds to the fraction of binary complexes in the samples ~3 × 10<sup>-4</sup> (mole ratio) (3, 7).

Subsequent annealing of the samples at 24 K gives rise to growth of a new series of eight infrared bands at 643, 698, 785, 1070, 1263, 1631, 3026, 3193 cm<sup>-1</sup> (see Fig. 1c; see also Fig. 2 for the deuterated analog). A simultaneous consumption of bands of isolated C<sub>2</sub>H<sub>2</sub>(C<sub>2</sub>D<sub>2</sub>) molecules is also observed. The sharp band of FO<sub>2</sub> radicals at 1490 cm<sup>-1</sup> grows in linear proportion to the new product bands and to the decrease of the 736.5 cm<sup>-1</sup> C<sub>2</sub>H<sub>2</sub> band, as shown in Fig. 3. This provides convincing evidence that this series corresponds to a primary reaction product of diffusing thermal F atoms with isolated C<sub>2</sub>H<sub>2</sub>.

In accordance with the gas-phase reaction [1], we might expect that both stereoisomers of 2-C<sub>2</sub>H<sub>2</sub>F radical and the C<sub>2</sub>H—HF complex could be formed in the reaction of thermally diffusing F atoms with C<sub>2</sub>H<sub>2</sub>. However, growth of the characteristic absorption bands of HF (4000–3500 cm<sup>-1</sup>) and C<sub>2</sub>H radical (1845 cm<sup>-1</sup>) (14) is not observed, signifying that excited 2-C<sub>2</sub>H<sub>2</sub>F radicals are efficiently stabilized in the argon matrix and do not decay by HF elimination to an observable extent. Each stereoisomer of 2-C<sub>2</sub>H<sub>2</sub>F radical has nine normal vibrations, and their most intense stretching vibrations C—F and C=C have comparable calculated intensities (see Table 1). However, in each spectral region a single absorption band is

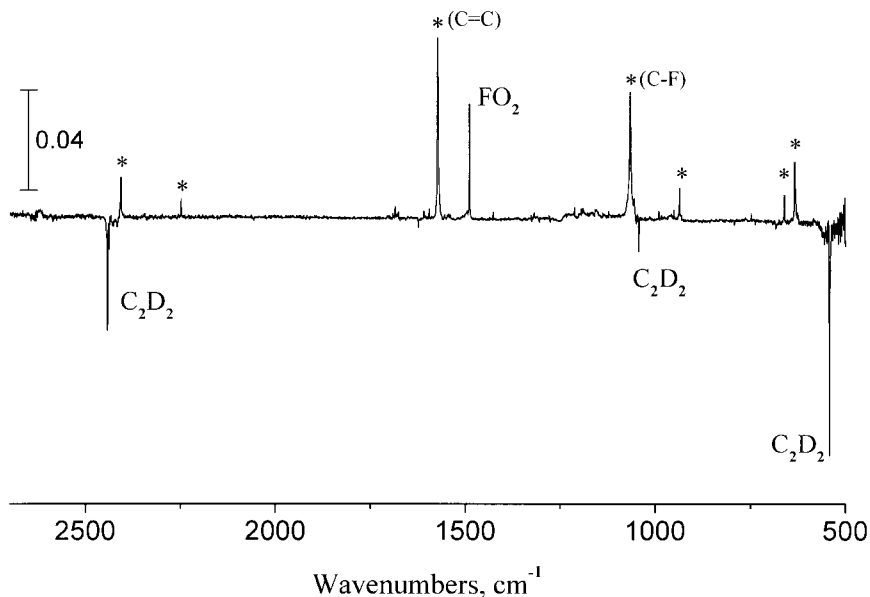


**FIG. 2.** Difference spectrum of photolyzed sample (Ar:F<sub>2</sub>:C<sub>2</sub>D<sub>2</sub> = 3000:1:1; C<sub>2</sub>H<sub>2</sub>-D<sub>2</sub>, 98 atom % D) before and after annealing at 24 K. IR bands of  $\beta$ -C<sub>2</sub>D<sub>2</sub>F are marked with asterisk. The spectrum was recorded at 15 K.

observed; hence, all of the new bands should be assigned to one isomer of 2-C<sub>2</sub>H<sub>2</sub>F. Experiments were carried out in which samples containing 2-C<sub>2</sub>H<sub>2</sub>F radicals were annealed at 30 K for 72 h, but no changes of the infrared spectra were observed. We therefore conclude that thermally activated *cis-trans* isomerization does not occur at this temperature. Thus, only one stereoisomer of 2-C<sub>2</sub>H<sub>2</sub>F radical is formed in the reaction of diffusing F atoms with isolated C<sub>2</sub>H<sub>2</sub>.

In samples containing higher F<sub>2</sub> concentration (Ar:F<sub>2</sub>:C<sub>2</sub>H<sub>2</sub> = 3000:3:1) two additional series of product bands appear upon annealing (see Fig. 4). The growth of these new bands exhibited a quadratic dependence with respect to the growth of FO<sub>2</sub> radicals, as shown in Fig. 3. This behavior is characteristic of secondary F atom addition products. The most intense bands of these secondary products are located at 877, 1153 cm<sup>-1</sup> and at 1129, 1714 cm<sup>-1</sup>. These bands were earlier

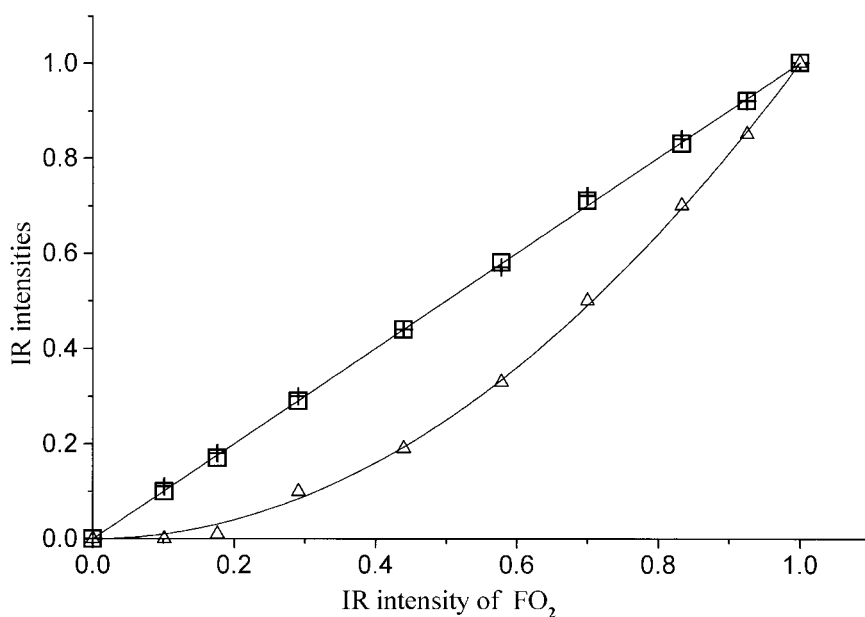


**FIG. 3.** Growth of (□) 2-C<sub>2</sub>H<sub>2</sub>F radical band (1631 cm<sup>-1</sup>) and consumption of the (+) C<sub>2</sub>H<sub>2</sub> band (736.5 cm<sup>-1</sup>) vs. intensity of the FO<sub>2</sub> (1490 cm<sup>-1</sup>) band during annealing of the photolyzed sample Ar:F<sub>2</sub>:C<sub>2</sub>H<sub>2</sub> = 3000:1:1. Increasing intensity of IR band of secondary product *cis*-CHF=CHF (1129 cm<sup>-1</sup>) in the sample Ar:F<sub>2</sub>:C<sub>2</sub>H<sub>2</sub> = 3000:3:1 is marked with Δ. All intensities of IR bands are shown with respect to their maximum value.

**TABLE 1**  
**Calculated Harmonic Frequencies (cm<sup>-1</sup>) and Isotropic hf**  
**Constants (mT) of Isomers of 2-Fluorovinyl Radical**

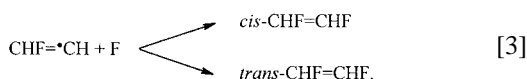
	<i>trans</i>		<i>cis</i>		exp. <sup>a</sup>		exp. <sup>b</sup>
1a' (CH <sup>a</sup> )	3307	(0.09)	3308	(0.13)	3193	(0.13)	3178
2a' (CH <sup>b</sup> )	3184	(0.01)	3122	(0.04)	3026	(0.04)	
3a' (CC)	1664	(0.48)	1678	(0.73)	1631	(0.71)	1623
4a' (H <sup>b</sup> CC)	1305	(0.01)	1291	(0.05)	1263	(0.11)	1211
5a' (CF)	1024	(1.00)	1093	(1.00)	1070	(1.00)	1066
6a' (H <sup>c</sup> CC)	779	(0.08)	734	(0.47)	698	(0.38)	678
7a' (FCC)	433	(0.00)	479	(0.04)			462
1a'' (wag)	883	(0.27)	827	(0.08)	785	(0.12)	785
2a'' (twist)	661	(0.28)	645	(0.42)	643	(0.40)	631
<i>a</i> <sub>F</sub>	10.12		6.69		6.50		7.3
<i>a</i> <sub>βH</sub>	1.69		3.81		3.86		3.81
<i>a</i> <sub>αH</sub>	0.14		0.17		0.25		--

Note. The relative intensities of vibrations are given in parentheses. Calculations were performed using the B3LYP/6-311++G(3df,2p) method and basis.

<sup>a</sup> This work.

<sup>b</sup> IR data are extracted from (14), while EPR are extracted from (13).

assigned to *trans*- and *cis*-1,2-difluoroethylene, respectively (19):



### B. EPR Spectrum of 2-C<sub>2</sub>H<sub>2</sub>F Radical

The EPR spectrum of a Ar:F<sub>2</sub>:C<sub>2</sub>H<sub>2</sub> = 3000:1:1 sample after UV photolysis at 15 K and subsequent annealing at 24 K is

shown in Fig. 5c. At temperatures below 20 K, the spectrum exhibits a series of anisotropic bands that are consistent with the spectrum previously reported by Cochran (11). At 30 K, the spectrum consists of eight narrow isotropic lines (the line-widths do not exceed 0.06 mT) having the same integrated intensities. Despite the different widths of the lines, all are components of hf structure of EPR spectrum of 2-C<sub>2</sub>H<sub>2</sub>F radical. There are three doublet hf splittings in the spectrum: *a*<sub>1</sub> = 6.50, *a*<sub>2</sub> = 3.86, and *a*<sub>3</sub> = 0.25 mT. The hf constants *a*<sub>1</sub> and *a*<sub>2</sub> are close to the literature values for 2-fluorovinyl radical (11, 13). However, the smallest splittings *a*<sub>3</sub> were not observed in previous studies. It was determined earlier that isotropic hf constant of the proton of α-CH group is nearly zero (20). Thus absence of splitting on α-H in the EPR spectra may result from insufficient resolution of the spectra caused by high concentration of the impurities or magnetic interactions with nuclei of the matrix. To demonstrate the influence of these effects on the spectral resolution, we have studied samples Ar:F<sub>2</sub>:C<sub>2</sub>H<sub>2</sub> = 300:1:1 and Kr:F<sub>2</sub>:C<sub>2</sub>H<sub>2</sub> = 3000:1:1 (nuclear spin of <sup>83</sup>Kr equals *I* = 9/2). In the first case (Fig. 5a), most of C<sub>2</sub>H<sub>2</sub> molecules are present in the sample as dimers (or larger clusters). Therefore 2-C<sub>2</sub>H<sub>2</sub>F radicals in this environment are formed adjacent to C<sub>2</sub>H<sub>2</sub> molecules, which cause line broadening due to incomplete averaging of anisotropic magnetic interactions. In the second case (Fig. 5b), strong line broadening results from interaction of unpaired electron with magnetic nuclei of the Kr matrix. Comparison of these spectra (5a and 5b) with the spectrum presented in the Fig. 5c shows that the highest spectral resolution is achieved in the argon matrix (nuclear spin of Ar is equal to zero) under conditions of perfect

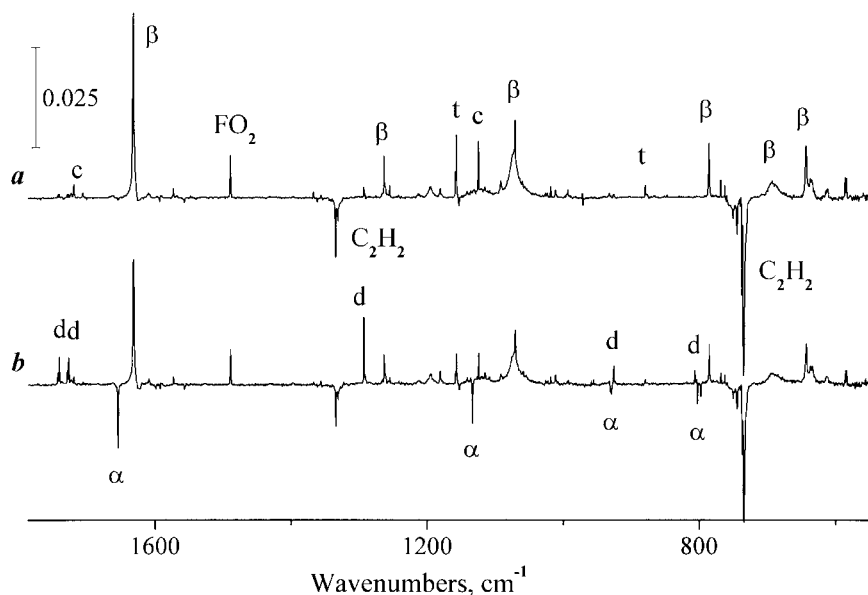


**FIG. 4.** Infrared spectra of secondary products in the Ar:F<sub>2</sub>:C<sub>2</sub>H<sub>2</sub> = 3000:3:1 sample: (a) after UV photolysis at  $\lambda = 355$  nm and partial annealing; (b) after successive visible light photolysis at  $\lambda = 532$  nm and final annealing. Spectra were recorded at 15 K.  $\beta$ , IR bands of CHF= $\dot{\text{C}}\text{H}$ ;  $\alpha$ , CH<sub>2</sub>= $\dot{\text{C}}\text{F}$ ; c, *cis*-CHF=CHF; t, *trans*-CHF=CHF; d, CH<sub>2</sub>=CF<sub>2</sub> species.

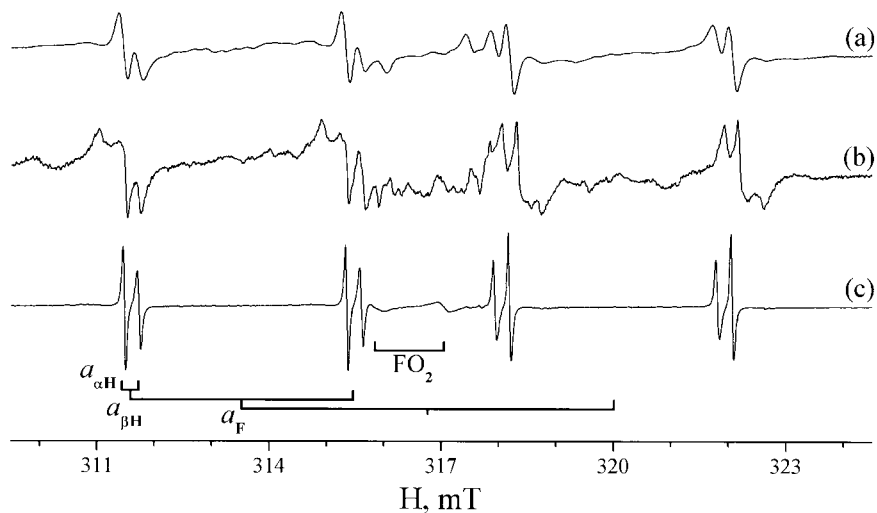


**FIG. 5.** EPR spectra of samples after photolysis at 15 K and subsequent annealing at 24 K: (a) Ar:F<sub>2</sub>:C<sub>2</sub>H<sub>2</sub> = 300:1:1; (b) Kr:F<sub>2</sub>:C<sub>2</sub>H<sub>2</sub> = 3000:1:1; (c) Ar:F<sub>2</sub>:C<sub>2</sub>H<sub>2</sub> = 3000:1:1. Spectra were recorded at 30 K.

isolation of stabilized radicals only. Fulfillment of this condition made it feasible to observe the smallest splitting  $a_3 = 0.25$  mT.

In order to distinguish between the hf constants on H and F nuclei, we have carried out a series of similar experiments with mixtures containing deuterium-enriched acetylene (75% C<sub>2</sub>D<sub>2</sub>, 22% C<sub>2</sub>HD, 3% C<sub>2</sub>H<sub>2</sub>). Addition of an F atom to C<sub>2</sub>D<sub>2</sub> gives rise to formation of CDF=·CD, whereas addition to C<sub>2</sub>HD

should form CHF=·CD and CDF=·CH radicals. Figure 6 shows the EPR spectrum of such a sample after low-temperature UV photolysis and subsequent annealing at 24 K. There are three series of lines in the spectrum. The first and dominant group of 2-C<sub>2</sub>D<sub>2</sub>F radical contains six lines: a doublet ( $a_1 = 6.50$  mT) of 1:1:1 triplets ( $a_2 = 0.59$  mT). The second series consists of four lines (CHF=·CD): doublet ( $a_1 = 6.50$  mT) of doublets ( $a_2 = 3.86$  mT). There are 12 lines (CDF=·CH) in

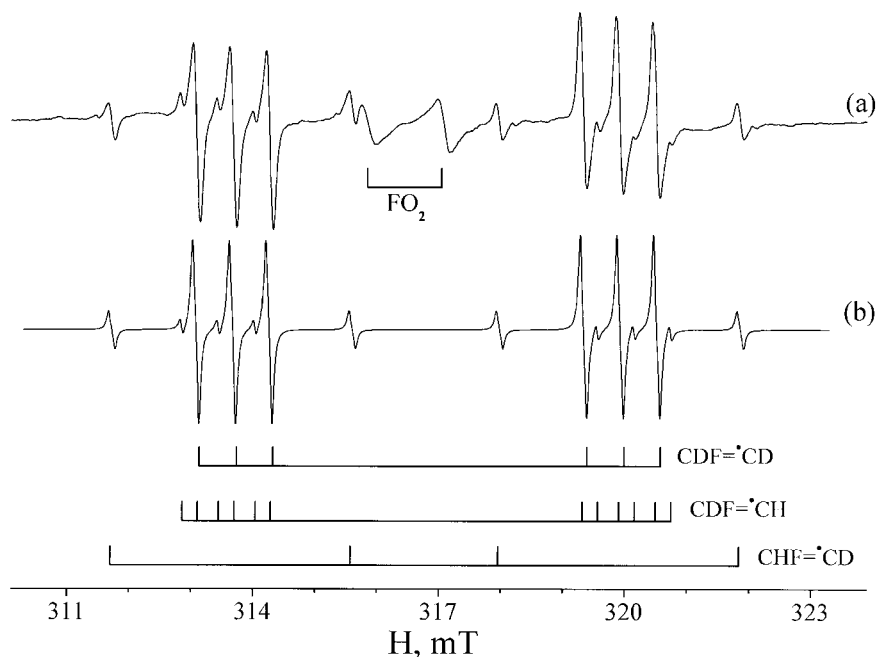


**FIG. 6.** (a) EPR spectrum of a sample Ar:F<sub>2</sub>:(C<sub>2</sub>D<sub>2</sub>(75%) + C<sub>2</sub>HD (22%) + C<sub>2</sub>H<sub>2</sub> (3%)) = 3000:1:1 after photolysis at 15 K and annealing at 24 K. The spectrum was recorded at 30 K. (b) Simulated spectrum of the sample containing radicals CDF=·CD (78%), CHF=·CD (11%), and CDF=·CH (11%), respectively. The hyperfine constants and linewidths are taken from the experimental spectrum (a).

the third group (six of them are masked by the more intense lines of the other series) formed from three hf splittings: two splittings on nonequivalent nuclei with spin  $I = \frac{1}{2}$  ( $a_1 = 6.50$  and  $a_3 = 0.25$  mT) and one splitting on a nuclear with spin  $I = 1$  ( $a_2 = 0.59$  mT). Upon H/D substitution, the hf splittings on proton nuclei should decrease by a factor of  $\gamma_H/\gamma_D \approx 6.5$  times due to the gyromagnetic ratios of the proton and deuteron. However, the hf splitting on  $^{19}\text{F}$  should be unchanged. Thus, the unchanged splitting  $a_1 = 6.50$  mT corresponds to hf splitting on  $^{19}\text{F}$ . The doublet splitting  $a_2 = 3.86$  mT in the radicals  $\text{CHF}=\dot{\text{C}}\text{H}$  and  $\text{CHF}=\dot{\text{C}}\text{D}$  and the triplet splitting  $a_2 = 0.59$  mT in  $\text{CDF}=\dot{\text{C}}\text{D}$  and  $\text{CDF}=\dot{\text{C}}\text{H}$  belong to hf splitting on the proton  $\beta$ -H. The remaining doublet splitting  $a_3 = 0.25$  mT ( $\text{CHF}=\dot{\text{C}}\text{H}$  and  $\text{CDF}=\dot{\text{C}}\text{H}$ ) must then be ascribed to the  $\alpha$ -H proton. The corresponding triplet splitting in the  $\text{CDF}=\dot{\text{C}}\text{D}$  and  $\text{CHF}=\dot{\text{C}}\text{D}$  radicals is less than the linewidth and could not be observed. Thus, in this study we were able to obtain a highly resolved EPR spectrum of 2- $\text{C}_2\text{H}_2\text{F}$  radical and to determine all its isotropic hf constants.

There are several well-known cases in which small radicals and molecules rotate in rare gas matrices almost freely (21, 22). If a radical rotates incoherently, the observed changes in the widths and intensities of the lines of EPR spectrum are explained by incomplete averaging of anisotropic magnetic interactions. Fraenkel and Freed (23) proposed a model of rotational diffusion based on the Redfield equations (24). This model draws an association between the linewidth of components of the hf structure and the distribution of electron density in the radical. In the case of a rapidly tumbling radical, the linewidth  $T_2^{-1}$  is described by

$$T_2^{-1} = T_{2,0}^{-1} + (A + \sum_i B_i m_i + \sum_i C_i m_i^2 + \sum_{i<j} E_{ij} m_i m_j) \tau_R, \quad [4]$$

where  $T_{2,0}^{-1}$  incorporates all contributions to linewidth that are not related to rotation;  $m_i$ ,  $m_j$  represent the  $z$  components of nuclear spin quantum number for nuclei  $i$  and  $j$ ;  $\tau_R$  is the rotational correlation time; and the coefficients  $A$ ,  $B$ ,  $C$ ,  $E$  are determined by anisotropic part of the hf interactions and  $g$  tensors. Since the EPR spectrum of  $\text{CHF}=\dot{\text{C}}\text{H}$  radical is symmetric and nuclear spins of all magnetic nuclei are  $I = \frac{1}{2}$ , only the cross term  $E_{ij} m_i m_j$  contributes to the difference in the linewidths. In the spectrum shown in Fig. 5c, lines with different signs of  $m_i m_j$  product for F and  $\alpha$ -H nuclei exhibit different widths. Therefore only the term  $E_{\text{FH}} m_{\text{F}} m_{\text{H}}$  contributes to the difference in linewidths. The coefficient  $E_{\text{FH}}$  arises from multiplication of hf interaction tensors (23, 25)

$$E_{\text{FH}} = \frac{8}{15} \hbar^2 \gamma_e^2 \gamma_{\text{F}} \gamma_{\text{H}} \sum_{k=-2}^{k=2} D_{\text{F}}^{(k)} D_{\text{H}}^{(-k)}, \quad [5]$$

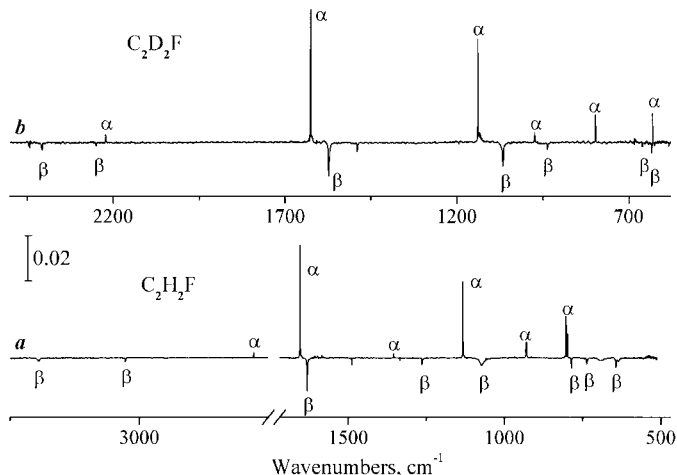


FIG. 7. Difference IR spectrum of UV photolyzed and annealed sample before and after photolysis at  $\lambda = 532$  nm; (a)  $\text{Ar}/\text{F}_2/\text{C}_2\text{H}_2$ ; (b)  $\text{Ar}/\text{F}_2/\text{C}_2\text{D}_2$ . IR bands of 2- $\text{C}_2\text{H}_2\text{F}$  and 1- $\text{C}_2\text{H}_2\text{F}$  are marked with  $\beta$  and  $\alpha$ , respectively. Spectra were recorded at 15 K.

where  $\gamma_e$  is the gyromagnetic ratio of electron;  $\gamma_{\text{F}}$ ,  $\gamma_{\text{H}}$  are the gyromagnetic ratios of nuclei of proton and fluorine; and

$$D_i^{(k)} = \sqrt{6\pi/5} \left\langle \Psi \left| \frac{Y_{2k}(\theta', \varphi')}{(r_i')^3} \right| \Psi \right\rangle$$

is the dipole-dipole interaction of the nuclear magnetic moment with the unpaired electron, averaged over its electronic wavefunction,  $\Psi$ . Based on the observed difference in linewidth,  $\Delta T_2^{-1} \cong 0.01$  mT at 30 K, we have estimated the rotational correlation time from Eqs. [4] and [5] to be  $\tau_R \sim 10^{-9}$  s.

### C. Photoinduced Conversions of 2- $\text{C}_2\text{H}_2\text{F}$ Radicals

Exhaustive photolysis of 2- $\text{C}_2\text{H}_2\text{F}$  radicals at  $\lambda = 532$  nm causes the intensities of the associated infrared absorption bands to decrease by about half. This change is accompanied by growth of a new series of six bands at 798(803), 930, 1133, 1355, 1654, 2778  $\text{cm}^{-1}$  (see Fig. 7a). In samples containing 2- $\text{C}_2\text{D}_2\text{F}$  radicals, the new bands are appeared at 630, 797, 973, 1138, 1625, 2221  $\text{cm}^{-1}$  (see Fig. 7b). This photoconversion was found to be reversible: subsequent short-time UV photolysis  $\lambda = 355$  nm leads to disappearance of new bands and to complete recovery of 2- $\text{C}_2\text{H}_2\text{F}$  radical bands. Figure 8 illustrates the kinetics of photoconversion under successive visible light and UV photolysis. From this figure, it is evident that changes in the intensities of infrared bands of 2- $\text{C}_2\text{H}_2\text{F}$  radical and new series of bands occur with the same photochemical rate. No changes are observed in intensities of others infrared bands.

Such a reversible photoconversion could be explained either by photoinduced *cis-trans* isomerization or by a structural

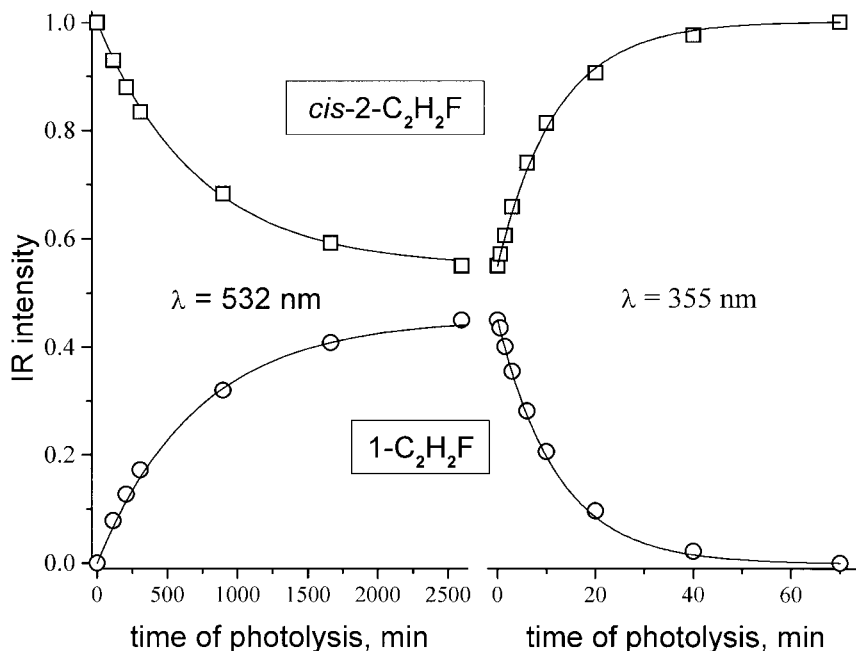


**FIG. 8.** Variation in IR band intensities of 2-C<sub>2</sub>H<sub>2</sub>F and 1-C<sub>2</sub>H<sub>2</sub>F radicals upon successive photolysis at  $\lambda = 532$  nm and  $\lambda = 355$  nm. Single exponential fits of experimental data are shown by solid curves. Characteristic times of 532- and 355-nm photolysis are equal to 715 and 12 min, respectively, at a photon flux of  $1.1 \times 10^{16} \text{ cm}^{-2} \text{ s}^{-1}$ .

isomerization 2-C<sub>2</sub>H<sub>2</sub>F  $\leftrightarrow$  1-C<sub>2</sub>H<sub>2</sub>F. It can be seen from Fig. 7 that bands in the region of the C—F (1133 cm<sup>-1</sup>) and C=C (1654 cm<sup>-1</sup>) stretching vibrations in the IR spectrum of the new radical have the greatest intensity, similar to the spectrum of 2-C<sub>2</sub>H<sub>2</sub>F radical. However, in the infrared spectrum of 2-C<sub>2</sub>H<sub>2</sub>F radical, the intensity of the C—F stretching band is nearly 50% higher than the C=C stretching band, whereas the new radical exhibits just the opposite behavior. In the C—H stretching region, the only observed band lies at 2778 cm<sup>-1</sup>, and its intensity is smaller than that of CH <sup>$\alpha$</sup>  vibration in 2-C<sub>2</sub>H<sub>2</sub>F radical by a factor of 10. These observations make it difficult to assign the new radical species to *trans*-2-C<sub>2</sub>H<sub>2</sub>F and instead favors an assignment to 1-C<sub>2</sub>H<sub>2</sub>F. A summary of the calculated vibrational frequencies and intensities are given in Table 1 (2-C<sub>2</sub>H<sub>2</sub>F), Table 2 (2-C<sub>2</sub>D<sub>2</sub>F) and Table 3 (1-C<sub>2</sub>H<sub>2</sub>F and 1-C<sub>2</sub>D<sub>2</sub>F).

The assignment of the new radical to 1-C<sub>2</sub>H<sub>2</sub>F was confirmed in experiments where F atoms were allowed to react with it to form 1,1-difluoroethylene



To accumulate a sufficient concentration of 1-C<sub>2</sub>H<sub>2</sub>F radicals, a partial annealing of a photolyzed sample at 24 K was performed. The temperature was then lowered to 15 K and the sample was subjected to a prolonged photolysis at  $\lambda = 532$  nm to convert half of the 2-C<sub>2</sub>H<sub>2</sub>F radicals to 1-C<sub>2</sub>H<sub>2</sub>F. The sample was then annealed until reactions of diffusing F atoms were

complete (as monitored by growth of the FO<sub>2</sub> band). Under these conditions fluorine atoms reacted not only with C<sub>2</sub>H<sub>2</sub> molecules and 2-C<sub>2</sub>H<sub>2</sub>F radicals, but also with the new 1-C<sub>2</sub>H<sub>2</sub>F radicals to form a new series of four bands at 806, 926, 1293, 1727(1741) cm<sup>-1</sup> that are in excellent agreement (apart from minor matrix shifts) with the vibrational frequencies of 1,1-difluoroethylene (19). This result definitively confirms that the new infrared spectrum that appears under 532 nm photolysis of 2-C<sub>2</sub>H<sub>2</sub>F radicals corresponds to 1-C<sub>2</sub>H<sub>2</sub>F radical.

**TABLE 2**  
Harmonic Frequencies (cm<sup>-1</sup>) and Isotropic hf Constants (mT) of Isomers of 2-Fluorovinyl-D<sub>2</sub> Radical

	<i>trans</i>	<i>cis</i>	exp.
1a' (CD <sup><math>\alpha</math></sup> )	2479 (0.12)	2474 (0.15)	2406 (0.12)
2a' (CD <sup><math>\beta</math></sup> )	2347 (0.01)	2300 (0.05)	2248 (0.05)
3a' (CC)	1590 (0.63)	1614 (0.86)	1572 (0.91)
4a' (D <sup><math>\beta</math></sup> CC)	1011 (1.00)	1074 (1.00)	1065 (1.00)
5a' (CF)	953 (0.05)	952 (0.10)	935 (0.10)
6a' (D <sup><math>\alpha</math></sup> CC)	701 (0.04)	649 (0.24)	633 (0.25)
7a' (FCC)	351 (0.)	396 (0.)	
1a'' (wag)	712 (0.06)	696 (0.01)	660 (0.04)
2a'' (twist)	530 (0.29)	488 (0.25)	
$a_{\text{F}}$			6.50
$a_{\beta\text{H}}$			0.59
$a_{\alpha\text{H}}$			<0.03

*Note.* The relative intensities of vibrations are given in parentheses. Calculations were performed using the B3LYP/6-311++G(3df,2p) method and basis.

**TABLE 3**  
**Calculated Harmonic Frequencies (cm<sup>-1</sup>) and Isotropic hf Constants (mT)**  
**for 1-Fluorovinyl and 1-Fluorovinyl-D<sub>2</sub> Radicals**

	CH <sub>2</sub> = <sup>•</sup> CF		CD <sub>2</sub> = <sup>•</sup> CF	
	calc.	exp.	calc.	exp.
1a' (CH <sup>1</sup> )	3236 (0.)		2406 (0.)	
2a' (CH <sup>2</sup> )	3111 (0.01)	2778 (0.01)	2278 (0.06)	2221 (0.04)
3a' (CC)	1701 (1.00)	1654 (1.00)	1669 (1.00)	1625 (1.00)
4a' (CH <sub>2</sub> bend)	1395 (0.04)	1355 (0.04)	995 (0.09)	973 (0.12)
5a' (CF)	1149 (0.51)	1133 (0.72)	1154 (0.55)	1138 (0.62)
6a' (rock)	943 (0.22)	930 (0.31)	808 (0.11)	797 (0.14)
7a' (FCC)	454 (0.)		393 (0.)	
1a'' (wag)	831 (0.33)	798 (0.41)	658 (0.18)	630 (0.19)
2a'' (twist)	615 (0.)		503 (0.)	
<i>a<sub>F</sub></i>	13.37	13.71		13.7
<i>a<sub>H1</sub></i>	4.16	4.21		0.65
<i>a<sub>H2</sub></i>	1.20	1.16		<0.05

*Note.* The relative intensities of vibrations are given in parentheses. Calculations were performed using the B3LYP/6-311++G(3df,2p) method and basis.

We performed similar EPR experiments and observed the reversible 532 nm photoconversion of 2-C<sub>2</sub>H<sub>2</sub>F radicals to 1-C<sub>2</sub>H<sub>2</sub>F radical. The EPR spectrum of the sample after completion of visible light photolysis is shown in Fig. 9. It consists of three doublet splittings which correspond to the hf structure from three nonequivalent magnetic nuclei with spin  $I = \frac{1}{2}$ . However, the new spectrum is more complex than EPR spectrum of CHF=•CH radical, since one of the hf splittings has an anisotropic component. The fact that this anisotropy is observed in 1-C<sub>2</sub>H<sub>2</sub>F and not 2-C<sub>2</sub>H<sub>2</sub>F is consistent with the relatively large contribution of *p* electron character introduced

by the F atom at the radical center. Based on H/D isotopic substitution we have determined hf splittings of 1-C<sub>2</sub>H<sub>2</sub>F:  $|A_{\perp}(F)| = 12.04$ ,  $|A_{\parallel}(F)| = 17.07$ , ( $a_F = [2 \cdot A_{\perp}(F) + A_{\parallel}(F)]/3 = 13.71$ ),  $a_{H1} = 4.21$ ,  $a_{H2} = 1.16$  mT. Notice that the isotropic hf constant on <sup>19</sup>F in this radical is more than twice as large as in 2-C<sub>2</sub>H<sub>2</sub>F radical.

#### D. Quantum-Chemical Calculations of Energy and Spectroscopic Characteristics of Fluorovinyl Radicals

All of calculations were performed using GAUSSIAN 98 suite of codes (26). It was demonstrated earlier that density

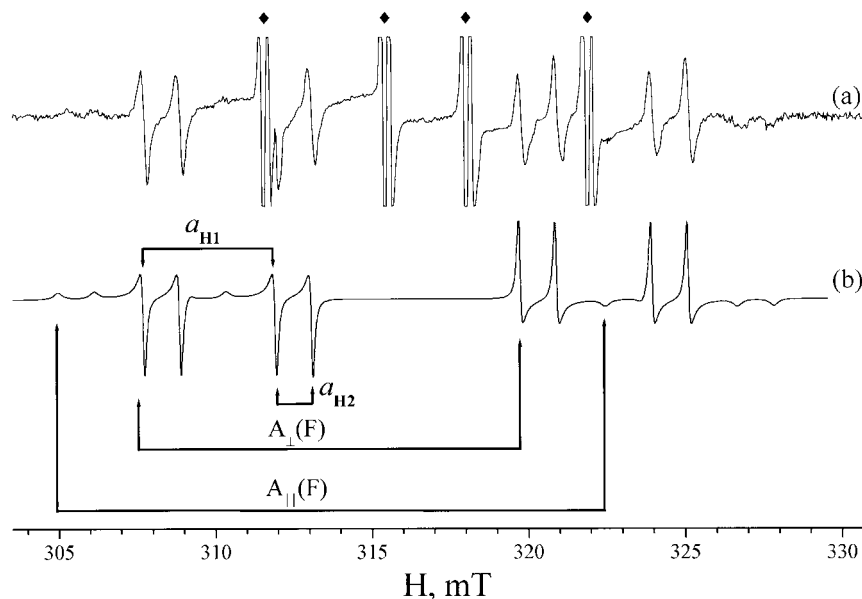


**FIG. 9.** (a) EPR spectrum of CH<sub>2</sub>=•CF radicals generated by 532-nm photolysis of CHF=•CH radicals. The spectrum was recorded at 30 K. Lines of CHF=•CH radicals are marked with diamonds. (b) Simulated spectrum using the experimentally measured linewidths and hyperfine splittings, as indicated.

**TABLE 4**  
**Optimized Geometries (Å and degrees) of Isomers of 2-Fluorovinyl Radical**

Parameter	<i>cis</i>			<i>trans</i>		
	B3LYP/ 6-311++G(d,p)	B3LYP/ 6-311++G(3df,2p)	QCISD/ 6-311++G(d,p)	B3LYP/ 6-311++G(d,p)	B3LYP/ 6-311++G(3df,2p)	QCISD/ 6-311++G(d,p)
R <sub>CH<math>\alpha</math></sub>	1.074	1.073	1.079	1.074	1.073	1.079
R <sub>CH<math>\beta</math></sub>	1.088	1.087	1.089	1.084	1.082	1.085
R <sub>CF</sub>	1.356	1.349	1.349	1.369	1.361	1.360
R <sub>CC</sub>	1.303	1.300	1.316	1.302	1.299	1.315
H $\alpha$ CC	139.9	139.5	136.0	144.5	144.1	140.1
H $\beta$ CC	125.6	125.2	125.2	125.9	125.6	125.8
FCC	122.9	123.2	122.5	122.8	122.9	122.1

functional (DF) theory calculations are able to accurately reproduce geometric, thermodynamic, and spectroscopic parameters of radicals at low computational cost (15, 27). Comparison with conventional post-Hartree–Fock methods shows that DF results are competitive with QCISD results for geometries and harmonic frequencies and with coupled cluster computations of hf interactions. We have used DF method B3LYP with 6-311++G(*d,p*) and 6-311++G(3df,2p) basis sets. There are no experimental data of geometries of fluorovinyl radicals. To assess the quality of the geometry predictions we have used results of computations at the QCISD/6-311++G(*d,p*) level of theory. The optimized geometries of stereoisomers of 2-fluorovinyl are compared for the different levels of calculations in Table 4. All methods gave similar bond lengths and bond angles, but the optimized geometry using the B3LYP/6-311++G(3df,2p) method is in better agreement with the QCISD calculations.

The next series of calculations was to obtain spectroscopic characteristics of the *cis* and *trans* isomers of 2-C<sub>2</sub>H<sub>2</sub>F radicals. The results of these calculations are compared with the experimental results in Table 1, and for deuterated radicals in Table 2. Agreement of the measured and calculated frequencies is somewhat better for the *cis* isomer than for *trans* isomer. However, a definitive assignment based only on these frequencies is not possible because the calculations do not account for effects of anharmonicity or frequency shifts due to the matrix environment. Table 1 illustrates that even slight changes in experimental conditions (i.e., Jacox's results (14) compared with this paper) can result in measurable differences in band positions.

Fortunately, a definitive assignment is possible based on a comparison of theoretical and measured isotropic hf constants. The calculations predict that the hf constants on F and  $\beta$ -H nuclei in *cis* and *trans* isomers strongly differ (values of  $a_F$  and  $a_{\beta H}$  differ more than 1.5 and 2 times, respectively). Good agreement of the calculated and measured values is obtained only for the *cis* isomer. Our previous studies (see (3, 4, 8)) and results of computations (15, 28) show that B3LYP method with appropriate basis set generally reproduces isotropic hf constants with ~5% accuracy. Therefore comparison of the calculated and measured hf constants of 2-C<sub>2</sub>H<sub>2</sub>F radicals allows

us to conclude that spectroscopic characteristics of stabilized radicals formed in the solid-state reaction of mobile F atoms with C<sub>2</sub>H<sub>2</sub> molecules correspond to those of *cis* isomer of 2-C<sub>2</sub>H<sub>2</sub>F radical.

Table 5 shows that the calculated energy of the *cis* isomer is lower than that of the *trans* isomer in all but the lowest level calculation. The energy difference is enhanced when the level of theory is increased and when zero-point vibrational energy (ZPE) is taken into account. At the highest level of theory the difference in the energies of isomers is 1.0 kJ/mol (1.5 kJ/mol with ZPE). Although such difference is comparable with the accuracy of energy calculations of isomers, the observed trends clearly indicate that the *cis* isomer is more stable than *trans* isomer. We have calculated the barrier of *cis*–*trans* isomerization; its height is only 9.0 kJ/mol. Thus, the equilibrium population of state of *trans* isomer at low temperatures  $T \leq 30$  K is extremely small. This conclusion is supported by our inability to detect the *trans* isomer (i.e., its population must be at least 20 times less than the *cis* isomer). From this limit, we calculate that the enthalpy of the *trans* isomer must be at least 0.7 kJ/mol higher than *cis*.

The calculated spectroscopic features of 1-C<sub>2</sub>H<sub>2</sub>F radical at B3LYP/6-311++G(3df,2p) level of theory are presented in Table 3. The calculated hf constants for 1-C<sub>2</sub>H<sub>2</sub>F radical are in excellent agreement with the experiments. Therefore, we have obtained dependable vibrational frequencies and hf constants of 1-C<sub>2</sub>H<sub>2</sub>F radical stabilized in solid argon for the first time.

**TABLE 5**  
**Calculated Difference in Electronic Energy,  $\Delta E_0 = E(\textit{trans}) - E(\textit{cis})$ , for 2-Fluorovinyl Radical Isomers with and without Zero-Point Energy Correction**

Method/Basis	$\Delta E_0$ , J/mol	$\Delta E_0 + \Delta ZPE$ , J/mol
B3LYP/6-311++G(d,p)	-95	336
B3LYP/6-311++G(2d,2p)	10	600
B3LYP/6-311++G(3df,2p)	859	1232
QCISD/6-311++G(d,p)	678	1174
G1	1100	1351
G2	1200	1489

## CONCLUSIONS

In this study we have shown that unambiguous identification of the isomeric form of fluorovinyl radicals can be accomplished using a combination of two complementary spectroscopic techniques, EPR and IR, along with quantum chemical calculations. The EPR technique plays the crucial role in the identification, since hyperfine constants are very sensitive to the geometry distortion of the open-shell species, and they can be precisely predicted by quantum-chemistry calculations. Reliable assignment of the vibrational frequencies of *cis*-2-C<sub>2</sub>H<sub>2</sub>F and 1-C<sub>2</sub>H<sub>2</sub>F radicals is made possible by the fact that the same reversible photoconversion of the two species is observed in both the EPR and IR experiments.

## ACKNOWLEDGMENTS

This research was supported by the U.S. National Science Foundation (Grant CHE-9970032) and the Russian Foundation for Basic Research (Grant 98-03-33175).

## REFERENCES

1. W. E. Jones and E. G. Skolnik, *Chem. Rev.* **76**, 563–591 (1976).
2. M. E. Jacox, *Rev. Chem. Intermed.* **6**, 77–120 (1985).
3. E. Ya. Misochko, V. A. Benderskii, A. U. Goldschleger, A. V. Akimov, A. V. Benderskii, and C. A. Wight, *J. Chem. Phys.* **106**, 3146–3156 (1997).
4. E. Ya. Misochko, I. U. Goldschleger, A. V. Akimov, and C. A. Wight, *Low Temp. Phys.* **26**, 727–735 (2000).
5. J. Feld, H. Kunttu, and V. A. Apkarian, *J. Chem. Phys.* **92**, 1009–1020 (1990).
6. E. Ya. Misochko, A. V. Akimov, and C. A. Wight, *Chem. Phys. Lett.* **293**, 547–554 (1998).
7. E. Ya. Misochko, A. V. Benderskii, and C. A. Wight, *J. Phys. Chem.* **100**, 4496–4502 (1996).
8. E. Ya. Misochko, V. A. Akimov, I. U. Goldschleger, A. I. Boldyrev, and C. A. Wight, *J. Am. Chem. Soc.* **121**, 405–410 (1999).
9. G. A. Kapralova, T. P. Nagornaya, and A. M. Chaikin, *Kinet. Katal.* **11**, 809–820 (1970); *Kinet. Katal.* 667–670 (1970).
10. R. L. Williams and F. S. Rowland, *J. Phys. Chem.* **77**, 301–310 (1973).
11. E. L. Cochran, F. J. Adrian, and V. A. Bowers, *J. Phys. Chem.* **74**, 2083–2089 (1970).
12. E. L. Cochran, F. J. Adrian, and V. A. Bowers, *J. Chem. Phys.* **40**, 213–219 (1964).
13. M. Shiotani, Y. Nagata, and J. Sohma, *J. Phys. Chem.* **86**, 4131–4137 (1982).
14. M. E. Jacox, *Chem. Phys.* **53**, 307–322 (1980).
15. V. Barone, C. Adamo, and N. Russo, *Chem. Phys. Lett.* **212**, 5–11 (1993).
16. E. Ya. Misochko, A. V. Akimov, and C. A. Wight, *Chem. Phys. Lett.* **274**, 23–28 (1997).
17. C. Zetsch, Ph.D. dissertation, Georg-August University, Göttingen, Germany, 1971.
18. G. R. Hunt and M. K. Wilson, *J. Chem. Phys.* **34**, 1301 (1961).
19. NIST Mass Spec Data Center, in “NIST Chemistry WebBook, NIST Standard Reference Database Number 69” (W. G. Mallard and P. J. Linstrom, Eds.), February 2000, National Institute of Standards and Technology, Gaithersburg, MD. [<http://webbook.nist.gov>]
20. H. M. McConnell and J. Strathdee, *Mol. Phys.* **2**, 129–138 (1959).
21. M. E. Jacox, *J. Mol. Spectrosc.* **66**, 272–287 (1977).
22. C. Girardet, L. Abouaf-Marguin, B. Gauthier-Roy, and D. Maillard, *Chem. Phys.* **89**, 415–430 (1984); *Chem. Phys.* **89**, 431–443 (1984).
23. J. H. Freed and G. K. Fraenkel, *J. Chem. Phys.* **39**, 326–348 (1963).
24. A. G. Redfield, *IBM Res. Dev.* **1**, 19–29 (1957).
25. J. H. Freed and G. K. Fraenkel, *J. Chem. Phys.* **40**, 1815–1829 (1963).
26. M. J. Frisch, G. W. Trucks, H. B. Schlegel, G. E. Scuseria, M. A. Robb, J. R. Cheeseman, V. G. Zakrzewski, J. A. Montgomery, Jr., R. E. Stratmann, J. C. Burant, S. Dapprich, J. M. Millam, A. D. Daniels, K. N. Kudin, M. C. Strain, O. Farkas, J. Tomasi, V. Barone, M. Cossi, R. Cammi, B. Mennucci, C. Pomelli, C. Adamo, S. Clifford, J. Ochterski, G. A. Petersson, P. Y. Ayala, Q. Cui, K. Morokuma, D. K. Malick, A. D. Rabuck, K. Raghavachari, J. B. Foresman, J. Cioslowski, J. V. Ortiz, B. B. Stefanov, G. Liu, A. Liashenko, P. Piskorz, I. Komaromi, R. Gomperts, R. L. Martin, D. J. Fox, T. Keith, M. A. Al-Laham, C. Y. Peng, A. Nanayakkara, C. Gonzalez, M. Challacombe, P. M. W. Gill, B. Johnson, W. Chen, M. W. Wong, J. L. Andres, C. Gonzalez, M. Head-Gordon, E. S. Replogle, and J. A. Pople, “GAUSSIAN 98, Revision A.3,” Gaussian, Inc., Pittsburgh, PA, 1998.
27. F. De Proft, J. M. L. Martin, and P. Geerlings, *Chem. Phys. Lett.* **250**, 393–397 (1996).
28. V. Barone, *J. Chem. Phys.* **101**, 6834–6838 (1994).